Superconductivity in amorphous T_5T_9 transition-metal alloys (T_5 = Nb, Ta; T_9 = Rh, Ir)

C. C. Koch, D. M. Kroeger, and J. O. Scarbrough
Metals and Ceramics Division, Oak Ridge National Laboratory, Oak Ridge, Tennessee 37830

B. C. Giessen
Materials Science Division, Institute of Chemical Analysis, Northeastern University, Boston, Massachusetts 02115

(Received 27 May 1980)

The superconducting transition temperature T_c has been measured for amorphous T_5T_9 alloys (where T_5 = Nb or Ta, T_9 = Rh or Ir) as a function of composition. Nb and Ta dominated the T_c behavior with T_c for Nb alloys $\approx 4.8-5.1$ K and T_c for Ta alloys $\approx 3.1-3.3$ K. Changing the average group number by varying the T_5/T_9 ratio had little effect on T_c within the ~ 10 at.% range of composition in which the amorphous alloys form. T_c decreased approximately linearly with x for $(Nb_{1-x}Ta_x)_{55}Rh_{45}$ and $(Nb_{1-x}Ta_x)_{55}Ir_{45}$. The electrical resistivity ρ_n and the upper critical field B_{c2} were measured as functions of temperature. The Sommerfeld constant γ was calculated from ρ_n and $dB_{c2}/dT|_{T_c}$ using the Ginzburg-Landau-Abrikosov-Gor'kov theory. The Debye temperature Θ_D was calculated from measurements of Young's modulus. The above parameters allowed calculations to be made of $N(E_F)$, the density of electronic states at the Fermi level, and λ, the electron-phonon coupling constant. It was found that λ more accurately reflected the T_c behavior than did $N(E_F)$ and that both electronic and phonon contributions had to be considered in the determination of λ.

I. INTRODUCTION

The first amorphous superconducting alloy obtained by rapid quenching from the liquid state, $La_{80}Au_{20}$, was reported in 1975.[1] Since then several dozen new liquid-quenched amorphous alloys have been discovered[2–4] which have added information to the field of amorphous superconductivity, first studied in vapor-quenched systems by Buckel and Hilsch.[5] Liquid-quenched alloys, which are typically 25–50 μm in thickness, provide bulk samples which are stable at room temperature and above, and thus can facilitate a variety of superconducting and physical property measurements not easily accomplished on thin films. Such measurements can also give information on the electronic structure of the amorphous alloys and contribute to the understanding of their formation and stability. Unfortunately, many of the transition-metal systems of interest can only be made amorphous from the liquid state by the addition of nontransition (metalloid) elements such as B, C, P, or Si. The presence of these metalloids complicates the electronic structure and the systematics of superconductivity in amorphous transition-metal alloys. Recently, a series of transition-metal–transition-metal binary alloys which consist of combinations of elements from column 5 and column 9 of the periodic table; i.e., Nb, Ta with Rh, Ir have been prepared in the amorphous form by quenching from the liquid. The alloys have been termed T_5T_9 alloys.[6] These amorphous alloys, produced by rapid quenching of the liquids are formed at compositions centered around approximately 45 at.% of the T_9 component, which corresponds to the composition where a eutectic is found in the equilibrium phase diagram.[7] The amorphous alloys fall at electron-to-atom ratios (e/a), as determined by the average group number in the periodic table, of ~ 6.6 to 7.0, a relatively favorable e/a for the occurrence of superconductivity in amorphous $4d$ and $5d$ transition metals.[8] However, since the components of the T_5T_9 alloys are not near neighbors in the periodic table it is expected that the superconducting transition temperatures T_c will fall below the curve of maximum T_c vs e/a determined by Collver and Hammond[8,9] on amorphous transition metals quenched from the vapor state. Collver and Hammond find that the degradation of T_c below their composite maximum T_c vs e/a curve is proportional to the difference in atomic number of the components.

One of the amorphous T_5T_9 alloys, $Nb_{55}Rh_{45}$, has been studied previously[10] with regard to its superconductivity and found to be superconducting below 4.7 K. No superconductivity measurements have been reported on the other amorphous alloys of this series.

In this paper we report superconductivity measurements of the T_5T_9 alloys as a function of composition, varying both e/a and the composition of the T_5 component. Measurements of T_c, the upper critical field $H_{c2}(T)$, and the normal-state resistivity ρ_n

allowed us to calculate the electronic coefficient of low-temperature specific-heat capacity, γ. Measurements of Young's modulus provided data for calculation of the Debye temperature, Θ_D. The values of Θ_D and T_c were then used to calculate the electron-phonon coupling constant, λ. With γ, and λ, values of the density of electronic states at the Fermi level $N(E_F)$ were calculated. The variation of T_c with $N(E_F)$ and λ, and the variation of an index of amorphous phase stability with $N(E_F)$ are presented and discussed.

II. EXPERIMENTAL

A. Sample preparation

The amorphous T_5T_9 alloys were prepared from high-purity Nb, Ta, Ir, and Rh. The Nb, Ta, and Ir were in the form of electron-beam melted rod; the Rh in the form of powder. Alloy buttons, ~3 g in weight, were made by arc melting the constituents together on a copper hearth in a partial pressure of purified argon. The buttons were turned over and remelted at least six times to maximize homogeneity. Where composition was to be varied in a given system, e.g., $(Nb_{1-x}Ta_x)_{55}Rh_{45}$, a master alloy, weighing approximately 10 g, was prepared first, sectioned, and the appropriate additions made. The alloys were broken into small sections and ~30-mg pieces were selected to be rapidly quenched from the melt. The rapid quenching was carried out in arc-hammer furnaces[6] at Northeastern University and Oak Ridge National Laboratory. Hammer velocities of ~5–6 m/s were used and the resulting foils obtained were typically 1 cm in diameter and 20–30 μm thick. A list of the alloys used in this study is given in Table I.

B. Sample characterization

X-ray diffraction patterns were made on all samples in order to determine their structure. All samples were surveyed in a Norelco vertical x-ray diffractometer using Ni-filtered Cu $K\alpha$ radiation. Selected samples were examined in more detail, again using Cu $K\alpha$ radiation but with a diffracted beam monochromator in the form of a graphite crystal.

The temperatures at which the amorphous phase transforms to a crystalline phase, or phases on heating, the crystallization temperature T_x were determined by differential thermal analysis, DTA. The DTA measurements were performed in a Mettler thermoanalyzer in an atmosphere of flowing purified argon at a heating rate of 10 °C/min. Pure platinum metal was used as the standard and equal weights of platinum standard and sample were used (~30 mg). The DTA apparatus calibration was checked by determining the melting points of pure Ag, Cu, and Al. Agreement of 1–2 °C was obtained with the accepted values.

C. Low-temperature measurements

Electrical resistance was measured by the four-probe technique using pressure-voltage contacts 4.876 mm apart on samples 8 to 10 mm long. The samples

TABLE I. Alloy composition and structure; a is 100% amorphous (to resolution of x-ray technique); $a+c$, some (minor) crystalline phase; c, mostly crystalline.

Alloy	Structure[a]	Alloy	Structure[a]
$Nb_{60}Rh_{40}$	$a+c$	$Ta_{59}Rh_{41}$	$a+c$
$Nb_{55}Rh_{45}$	a	$Ta_{55}Rh_{45}$	a
$Nb_{50}Rh_{50}$	$a+c$	$Ta_{51}Rh_{49}$	a
$Nb_{57}Ir_{43}$	a	$Ta_{60}Ir_{40}$	a
$Nb_{55}Ir_{45}$	a	$Ta_{55.5}Ir_{44.5}$	a
$Nb_{53}Ir_{47}$	a	$Ta_{55}Ir_{45}$	a
$Nb_{50}Ir_{50}$	$a+c$	$Ta_{50}Ir_{50}$	a
$Nb_{48}Ir_{52}$	c	$(Nb_{1-x}Ta_x)_{55}Ir_{45}$	
		$x=0.25$	a
$Nb_{44}Ir_{36}B_{20}$	$a+c$	$x=0.50$	a
$Nb_{40}Ir_{40}B_{20}$	a	$x=0.75$	a
		$(Nb_{1-x}Ta_x)_{55}Rh_{45}$	
$Nb_{38.4}Ir_{41.6}B_{20}$	a	$x=0.25$	a
		$x=0.50$	a
		$x=0.75$	a

[a]Structure by x-ray diffraction.

were cut from the quenched disks by mounting the disks in wax and using a diamond slitting saw positioned by a micrometer. The samples were typically 8–10 mm long, 1.0 to 1.3 mm wide, and 25 to 30 μm thick. The chief source of error in determining the form factor for calculating resistivity from the resistance measurements comes from the thickness measurements. The average value of resistivity and the standard deviation were estimated for alloys where more than one sample was made and measured. The electrical resistance was measured from room temperature down through the superconducting transition temperature. A Chromel-Au-0.07 at.% Fe thermocouple was used as a temperature probe over the entire temperature range. Near T_c, a calibrated Ge resistance thermometer was employed to give a more precise measurement of T_c. A Keithley milliohmmeter model 503 was used for the resistance measurements.

T_c was measured both resistively, as described above, and by an ac susceptibility method. Good agreement was observed between results obtained by both techniques. A calibrated Ge thermometer was used as a temperature probe in the ac susceptibility method and a pure lead sample was kept in one of the measuring coils, its T_c serving as an internal calibration check. The pressure above the helium bath was reduced to obtain temperatures below 4.2 K and the vapor pressure of the helium provided another temperature comparison with the Ge thermometer calibration. Differences of less than 10 mK were always observed between the two temperature measurements.

The upper critical field H_{c2} was measured as a function of temperature by the resistive technique. A temperature was set, e.g., by controlling the helium vapor pressure, and the magnetic field produced by a 7-T superconducting solenoid was swept.

D. Elastic constant measurements

Young's modulus was measured on $Nb_{55}Rh_{45}$, $Nb_{55}Ir_{45}$, $Ta_{55}Rh_{45}$, and $Ta_{55}Ir_{45}$ by the technique of impulse-induced resonance at Northeastern University. This technique has been described recently[11] and shown to be accurate to $\approx 0.4\%$ in Young's modulus for samples similar to those used in the present work.

III. DISCUSSION OF EXPERIMENTAL RESULTS

A. Structure

The results of the x-ray diffraction measurements on all alloys are summarized in Table I. Alloys for which no Bragg peaks could be resolved are labeled *a* while those for which some crystalline peaks were observed are labeled $a+c$. The amorphous phase was always the majority phase (with the exception of $Nb_{48}Ir_{52}$ which was mostly crystalline and labeled *c*). An example of the x-ray diffraction results is presented in Fig. 1 for a $Ta_{55}Ir_{45}$ alloy where the intensity is plotted against the scattering angle 2θ. The major features of this diffraction pattern were identical for all the amorphous alloys studied. The second peak exhibits a definite splitting. The scattering vector $K = 4\pi \sin\theta/\lambda$ was calculated with λ the x-ray wavelength (Cu $K\alpha$). The first maximum in intensity, $I(K)$ occurred at $K = 27.7$ nm^{-1} (2.77 Å^{-1}) for all alloys, to within experimental accuracy, giving a value for the average nearest-neighbor distance (from either the Ehrenfest formula[12] or the conventional approximation[13] of $d = 0.278$ nm (2.78 Å). The similarity of the diffraction patterns for these alloys is understandable since the atomic diameters of Nb and Ta are nearly identical and those for Rh and Ir differ by only $\sim 1\%$. It was found that the ability to produce a completely amorphous sample decreased on either side of the composition at which the $e/a = 6.8$. This composition is the eutectic composition. At this e/a it was observed that the ease of glass formation, in terms of the hammer velocity (quench rate) required to produce the completely amorphous structure, increased in the order $Nb_{55}Rh_{45}$, $Ta_{55}Rh_{45}$, $Nb_{55}Ir_{45}$, $Ta_{55}Ir_{45}$. Only the very fastest hammer speeds produced completely amorphous $Nb_{55}Rh_{45}$. This trend is also reflected in the relative stability of the amorphous phase and will be discussed later in this paper.

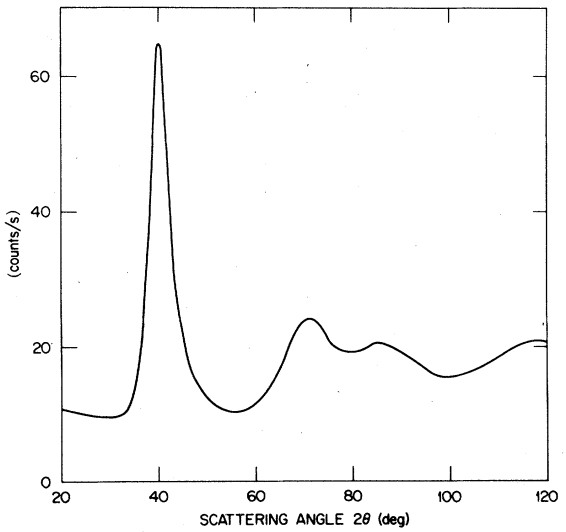

FIG. 1. Diffracted intensity vs scattering angle for $Ta_{55}Ir_{45}$.

TABLE II. Crystallization temperatures.

Alloy	T_x[a] (K)	Heating rate (K/min)	T_x[b] (K)	Heating rate (K/min)
$Nb_{55}Rh_{45}$	951 ± 10	10	973 ± 10	8
$Ta_{55}Rh_{45}$	1151 ± 10	10	1118 ± 10	3
$Nb_{55}Ir_{45}$	1168 ± 10	10	1133 ± 10	3
$Ta_{55}Ir_{45}$	1338 ± 10	10	1283 ± 10	1

[a]Present work. [b]Davis *et al.* (Ref. 14).

B. Crystallization temperatures

The crystallization temperatures T_x, determined by DTA are listed in Table II for the four T_5T_9 amorphous alloys. T_x values determined by changes in electrical resistance by Davis *et al.*[14] are also listed in Table II. Since T_x is a kinetic parameter dependent on heating rate, comparisons should be made for T_x values determined at constant heating rate. The variation of T_x with heating rate is shown in Fig. 2 for the $Ta_{55}Ir_{45}$ alloy, along with the T_x value from Davis *et al.* If the heating rate variations are taken into account then the present data agree with those of Davis *et al.* to within 10–15 K. These differences may be attributed to compositional variations, unresolved crystalline nucleation sites, etc. The order for T_x [i.e., $T_x(Ta_{55}Ir_{45}) > T_x(Nb_{55}Ir_{45}) > T_x(Ta_{55}Rh_{45}) > T_x(Nb_{55}Rh_{45})$] in the T_5T_9 alloys was identical in the two experiments.

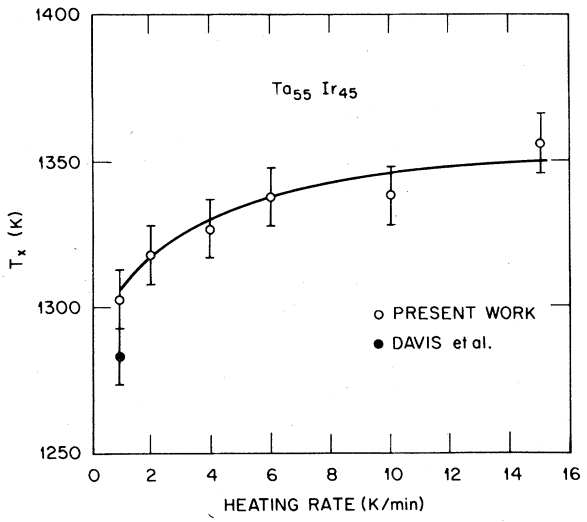

FIG. 2. Crystallization temperature T_x vs heating rate in DTA apparatus for $Ta_{55}Ir_{45}$.

C. Superconducting transition temperatures

T_c is plotted against e/a in Fig. 3 for the four T_5T_9 alloy systems. There would appear to be very little variation of T_c with e/a in these amorphous alloys although there is an indication of a small increase of T_c with decreasing e/a. This later trend in T_c vs e/a is consistent with the observations of Collver and Hammond[8] on vapor-deposited amorphous transition-metal alloys. The T_c data for the T_5T_9 alloys are compared to the Collver and Hammond data for Mo-Ru and Mo-Re amorphous alloys in Fig. 3. The magnitude of T_c variation with decreasing e/a is much less for the T_5T_9 alloys and

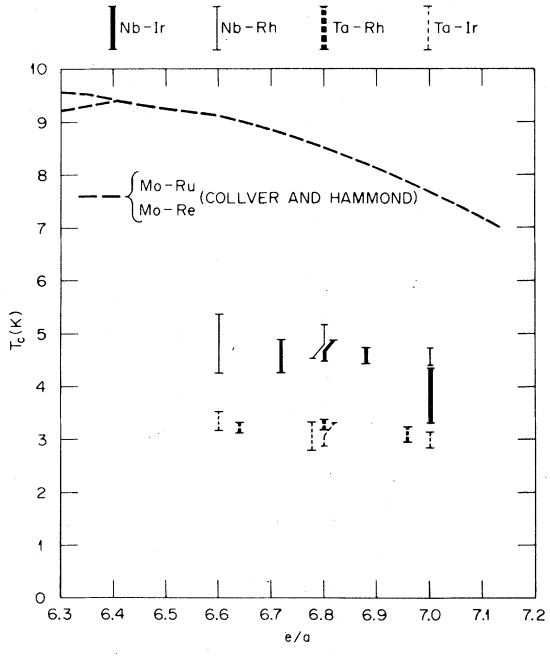

FIG. 3. Superconducting transition temperature T_c vs electron-to-atom ratio (average group number), e/a.

the T_c values fall well below the curve for amorphous Mo-Ru and Mo-Re. Collver and Hammond[9] noted that vapor-deposited amorphous transition-metal alloys do not follow a "universal curve" for T_c vs e/a if the alloys are composed of transition-metal elements widely separated in the periodic table. It was suggested[9] that the lower T_c's observed in amorphous alloys made from elements on opposite sides of the half filled d band were due to "charge transfer." It was proposed that this charge transfer may produce a local ordering which might reduce T_c by reducing the number of nearest neighbors. This suggestion is very speculative. The "rigid-band" model, which might be envoked to describe the "universal" T_c vs e/a curve for near neighbors in the periodic table,[8] apparently breaks down for alloys composed of constituents removed from one another in the periodic table.[9] Since the rigid-band concept is inapplicable, the specific normal-state electronic and lattice properties of a given alloy must be considered in order to explain T_c.

The widths of the transition ΔT_c from the normal to the superconducting state are noted (Fig. 3) to vary from < 0.2 to > 1.0 K. The largest ΔT_c's are observed near the boundary of the composition range where the amorphous phase is formed, i.e., in alloys with some fraction of crystalline material. The largest ΔT_c values are seen for $Nb_{60}Rh_{40}$ and $Nb_{50}Ir_{50}$ alloys (Fig. 3). The crystalline phase existing close to $Nb_{60}Rh_{40}$ in the equilibrium phase diagram is a σ phase with $T_c = 4.04$ K.[15] The ΔT_c in the present study extends from 5.39 to 4.26 K. Thus, the completion of the transition is still above T_c for the equilibrium σ phase. However, a metastable crystalline phase with $T_c > 4.04$ K or the influence of the amorphous matrix via the proximity effect might indicate a higher T_c for the minor crystalline phase. Conversely, the ΔT_c might be unrelated to the small fraction of crystalline second phase but be due to composition gradients in, perhaps, interstitial impurities such as oxygen. It has been shown that interstitial content can have a marked effect on T_c in the crystalline phases in Nb-Ir alloys.[16] Similar speculation applies to the $Nb_{50}Ir_{50}$ alloy where the equilibrium, α_1 (tetragonal), or metastable α_2 (orthorhombic), crystalline phases have T_c values ~ 4 K.[17] Rapidly quenched $Nb_{48}Ir_{52}$ alloys were found to have the α_2 orthorhombic crystal structure so that the traces of crystalline material in $Nb_{50}Ir_{50}$ are most likely this phase. The equilibrium crystaline phases in the Ta-Rh system in the composition range of interest have T_c values of 2.0 to 2.35 K,[15,18] while superconductivity has not been observed in the equilibrium phases of the Ta-Ir system at these compositions down to 1.2 K.[15,18] Metastable crystalline phases have been obtained by rapid quenching for $Nb_{55}Ir_{40}O_5$, $Ta_{54}Rh_{43}C_3$, and $Ta_{58}Ir_{42}$ with T_c values of 10.5, 10, and 6.6 K, respectively.[19] Thus, the amorphous T_5T_9 alloys

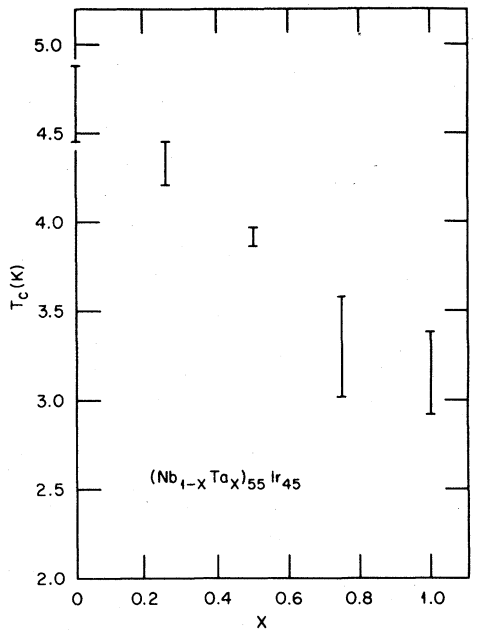

FIG. 4. Superconducting transition temperature T_c vs x in $(Nb_{1-x}Ta_x)_{55}Ir_{45}$.

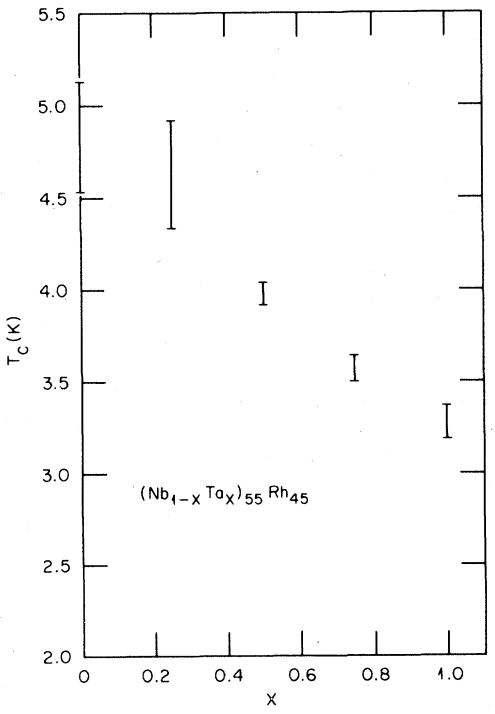

FIG. 5. Superconducting transition temperature T_c vs x in $(Nb_{1-x}Ta_x)_{55}Rh_{45}$.

have T_c values comparable to (Nb-base alloys) or greater than (Ta-base alloys) those of the corresponding equilibrium crystalline phases. However, metastable crystalline phases stabilized by interstitial impurities can have much higher T_c values.

Boron was added to Nb-Ir alloys in a preliminary study of the influence of metalloid additions to this system. The following alloys were prepared: $(Nb_{0.55}Ir_{0.45})_{80}B_{20}$, $(Nb_{0.50}Ir_{0.50})_{80}B_{20}$, and $(Nb_{0.48}Ir_{0.52})_{80}B_{20}$. The $(Nb_{0.55}Ir_{0.45})_{80}B_{20}$ alloy was found by x-ray diffraction to be mixed amorphous and crystalline while the other two alloys were completely amorphous. Therefore, B apparently shifts the glass-forming compositions to higher Ir content in the Nb-Ir system. The presence of B reduced the T_c of the amorphous phase to 2.89 K (with ΔT_c extending to 2.32 K). The decrease of T_c with metalloid additions has also been observed in a systematic study of amorphous $Mo_{0.6}Ru_{0.4}$ alloys by Johnson and Williams.[20]

The T_c values resulting from substitution of Ta for Nb in $(Nb_{1-x}Ta_x)_{55}Ir_{45}$ and $(Nb_{1-x}Ta_x)_{55}Rh_{45}$ are shown in Figs. 4 and 5, respectively. An almost linear decrease in T_c is observed as Ta replaces Nb in these alloys.

D. Upper critical field H_{c2}

The upper critical field $H_{c2} \approx B_{c2}$ is plotted versus T_c in Fig. 6 for $Ta_{55}Rh_{45}$ and $Nb_{55}Ir_{45}$ as examples typical of all the data. An extended linear region of $B_{c2}(T)$ is observed. Such linear $B_{c2}(T)$ data are commonly observed in the amorphous superconductors studied to date[3] and the magnitudes of $dB_{c2}(T)/dT|_{T_c}$ are also comparable. These values are also similar to those observed for "dirty" (short mean free path) crystalline transition-metal alloys.[21] The values for $dB_{c2}(T)/dT|_{T_c}$ were similar for all the alloys measured at about 2.5 T/K.

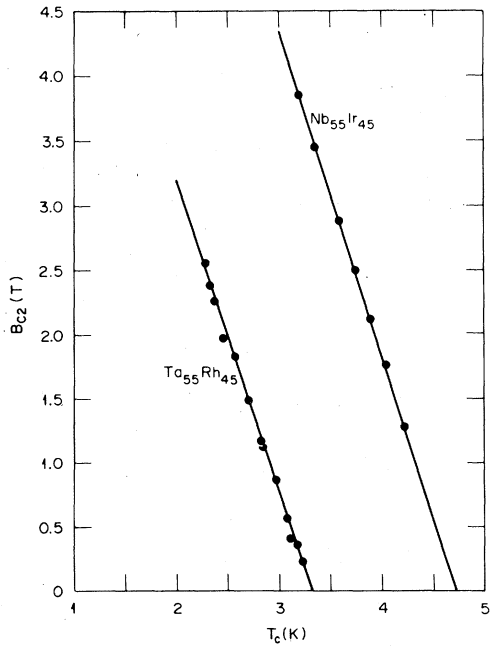

FIG. 6. Upper critical field $B_{c2}(T)$ vs temperature for $Ta_{55}Rh_{45}$ and $Nb_{55}Ir_{45}$.

E. Electrical resistivity

The electrical resistivity measured at 10 K is plotted against composition x in Fig. 7 for the $(Nb_{1-x}Ta_x)_{55}Rh_{45}$ and $(Nb_{1-x}Ta_x)_{55}Ir_{45}$ alloys. Substitution of Ta for Nb in these alloys increases the

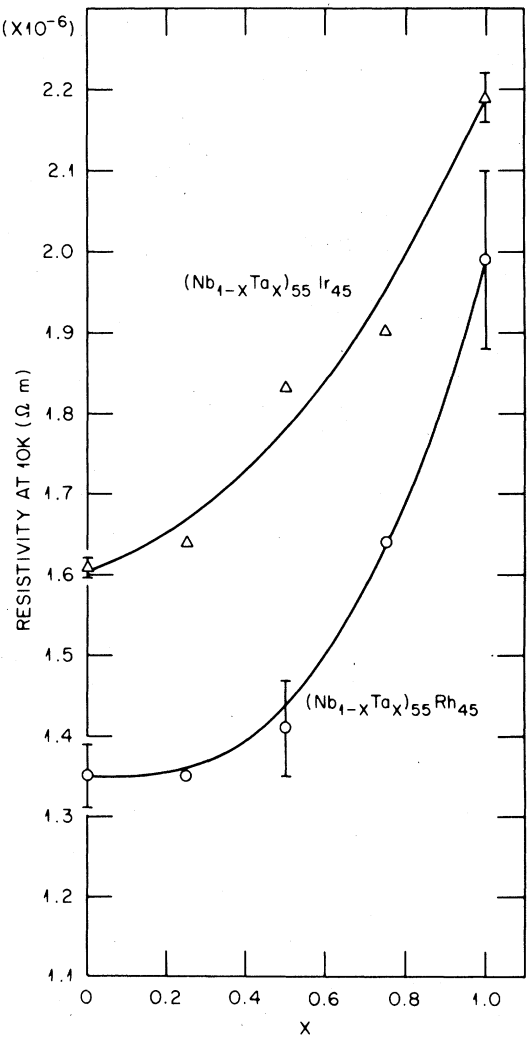

FIG. 7. Resistivity at 10 K vs x for $(Nb_{1-x}Ta_x)_{55}Ir_{45}$ and $(Nb_{1-x}Ta_x)_{55}Rh_{45}$.

resistivity and the Ir containing alloys have higher resistivities than the Rh alloys at a given value of x. Resistivity increased slightly as the measuring temperature was lowered such that all alloys exhibited a negative temperature coefficient (NTC) of resistivity, $(1/\rho_n)(d\rho_n/dT)$. The magnitude of the NTC increased with resistivity so that $Nb_{55}Rh_{45}$ had the smallest NTC and $Ta_{55}Ir_{45}$ the largest. The temperature coefficient of resistivity is plotted against composition in Fig. 8.

Explanations of resistivity in amorphous alloys have been based on the Ziman-Faber theory[22] for the resistivity of simple liquid metals and its extension to liquid transition metals.[23] The electrical resistivity of liquid or amorphous binary transition-metal alloys of components A, B is given by[23]

$$\rho = C(K_F)\int^{2K_F} |u(K)|^2 K^3\, dK \ , \tag{1}$$

with

$$\begin{aligned} |u(K)|^2 = {} & C_A|t_A|^2(1-C_A+C_A a_{AA}) \\ & + C_B|t_B|^2(1-C_B+C_B a_{BB}) \\ & + C_A C_B(t_A^* t_B + t_A t_B^*)(a_{AB}-1) \ , \end{aligned} \tag{2}$$

and C_A, C_B are the concentrations, t_A, t_B are the t matrices of components A and B, and a_{AA}, a_{AB}, and a_{BB} are the partial structure factors of the alloy. Except for concentration, none of these quantities are known for the T_5T_9 alloys. However, if it is assumed that the substitution of Ta for Nb does not change the partial structure factors (the atomic diameters of Ta and Nb are nearly equal) then an explanation for the increase in ρ_n due to this substitution can be given in terms of the resonant scattering of the conduction electrons by the d states lying in the conduction band. Such an argument is given by Stocks[24] as follows. The phase shifts were calculated for Ta and Nb using self-consistent $X\alpha$ potentials from Papaconstantopoulos and Klein.[25] Likewise, the imaginary part of the scattering amplitude

$$\sin^2 2\alpha \frac{\Gamma^2}{\Gamma^2 + 4(E_{\rm res}-E_F)^2}$$

was calculated with the same potential functions. Here Γ is the width and $E_{\rm res}$ the energy of the scattering resonance. Fermi energies for Nb and Ta in the T_5T_9 alloys were estimated assuming a rigid band with $e/a = 6.8$ and the integrated density of states determined by Mattheiss[26] for Nb and Ta. In both cases E_F was above $E_{\rm res}$ and the scattering amplitude for Ta was $\sim 20\%$ higher than for Nb. This is due to the fact that $\Gamma(\mathrm{Ta}) > \Gamma(\mathrm{Nb})$ and $(E_{\rm res}-E_F)_{\rm Ta} < (E_{\rm res}-E_F)_{\rm Nb}$.

However, the extended Ziman-Faber theory has been recently reexamined[27] from a consistent application of the single-site approximation. The conclusions from this study indicate that the Ziman-Faber theory greatly overestimates the resistivity in strong scattering systems and in general the results are very sensitive to the choice of effective free-electron parameters.

Within the limits of this model, however, the above rationalization of the T_5T_9 resistivity data assumed that neither the partial structure factors nor the other terms in Eq. (2) change significantly on substitution of Ta for Nb. It is planned[28] to use the T_5T_9 amorphous alloys as a model system where measurements of the structure factors can be combined with detailed cluster calculations to obtain the parameters needed to test the Ziman-Faber model.

The NTC of resistivity and its magnitude have also been qualitatively explained by the Ziman-Faber model. According to this model the largest resistivity and NTC should both occur when $2K_F \approx K_p$, where $2K_F$ is the "spanning vector" of the Fermi surface and K_p is the position of the first maximum in $S(k)$, the structure factor. The broadening of the $S(k)$ peak at K_p with temperature causes the NTC. This behavior has been observed in many amorphous alloys and is noted in the present study in that both ρ_n and NTC increase with x in $(Nb_{1-x}Ta_x)_{55}Ir_{45}$ and $(Nb_{1-x}Ta_x)_{55}Rh_{45}$.

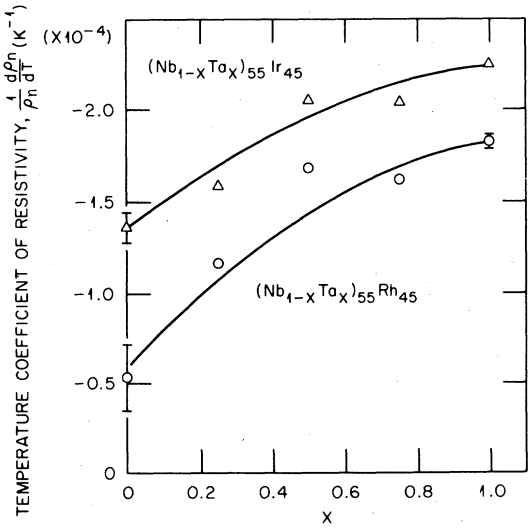

FIG. 8. Temperature coefficient of resistivity vs x for $(Nb_{1-x}Ta_x)_{55}Ir_{45}$ and $(Nb_{1-x}Ta_x)_{55}Rh_{45}$.

F. Calculation of electronic density of states at the Fermi level $N(E_F)$

1. *Calculation of the Sommerfeld constant* γ

The electronic coefficient of low-temperature specific heat γ can be calculated according to the

Ginzburg-Landau-Abrikosov-Gor'kov (GLAG) theory[29] by the following expression:

$$\gamma = -\frac{\pi^3}{12}\frac{k_B}{e}\frac{1}{\rho_n}\frac{dB_{c2}}{dT}\bigg|_{T_c}, \tag{3}$$

where k_B is the Boltzmann constant and e is the electron charge. This expression should be applicable near T_c and in the dirty limit, i.e., where the electron mean free path is much less than the superconducting coherence length. This criterion is met by all the T_5T_9 alloys since the mean free path is 0.3–0.4 nm and the coherence length is 6.0–7.0 nm for $T \ll T_c$. The general validity of this expression as applied to transition-metal alloys has been questioned.[30] It was suggested that Eq. (3) is inapplicable in alloys with d and s electrons because the transport mean free path is determined mainly by s electrons while superconducting properties are controlled by the d electrons. This suggestion is questionable since, while clearly the s electrons carry the current, the dominant scattering is from the d electrons which determine the resistivity in transition metals. Furthermore, for elements to the left of Pd in the periodic table, such as the T_5T_9 alloys, there is sufficient hybridization of the s and d electrons[31] to make separate descriptions of s and d bands unlikely. The ultimate test of Eq. (3) is its agreement with experimental results. The literature was searched for alloys where the quantities in Eq. (3) had been measured and where measurements of γ from low-temperature specific heat capacity are available. In Fig. 9, γ calculated from the GLAG theory is plotted against experimentally determined γ values for crystalline compounds, alloys, and amorphous alloys. Even though vapor-deposited V_3Si and Nb_3Sn do not meet the dirty-limit criterion,[32] good agreement is observed. High-resistivity crystalline Ti-base alloys[21] exhibit excellent agreement. Amorphous La-Ga alloys[33] conform to the γ calculated by the GLAG theory while La_{76}-Au_{24} does not show good agreement.[34] However, if more recent[35] (lower) resistivity data are used for $La_{76}Au_{24}$, better agreement is observed. In general, the available data would seem to strongly support the validity of Eq. (3).

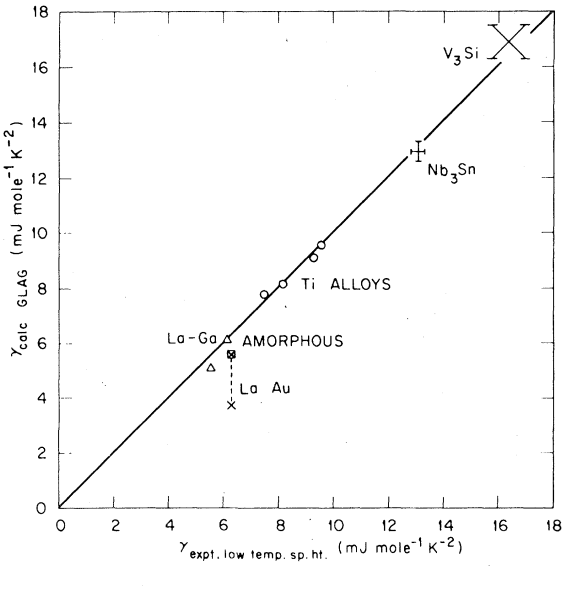

FIG. 9. γ calculated from the GLAG theory vs γ measured in low-temperature specific-heat-capacity experiments. References given in text.

While direct measurements of γ are not available, resistivity and superconducting property measurements on $(Mo_{0.6}Ru_{0.4})_{1-x}Si_x$ (Ref. 20) and $(Mo_{1-x}Ru_x)_{80}P_{20}$ (Ref. 36) alloys do not appear to be consistent with Eq. (3). That is, γ calculated from the GLAG theory was essentially constant with x in $(Mo_{1-x}Ru_x)_{80}P_{20}$ even though T_c and $N(E_F)$ (estimated from magnetic-susceptibility data) both decrease with x. The γ calculated for $(Mo_{0.6}Ru_{0.4})_{1-x}Si_x$ increased with x while T_c was decreasing. Thus, either the validity of Eq. (3) has been violated in these systems or T_c is controlled by some factor other than $N(E_F)$. It may be significant that both these systems contain metalloid elements.

2. *Calculation of the electron-phonon coupling constant* λ

One of the most important parameters in the theory of superconductivity is the electron-phonon coupling constant λ. The λ can be calculated from the McMillan equation[37]

$$\lambda = \frac{1.04 + \mu^* \ln(\Theta_D/1.45T_c)}{(1-0.62\mu^*)\ln(\Theta_D/1.45T_c) - 1.04}, \tag{4}$$

where μ^* is the Coulomb pseudopotential and Θ_D is the Debye temperature. The value for μ^* is not known but typically values of 0.1 to 0.2 are used. We used both $\mu^* = 0.1$ and 0.15. The latter value is consistent with estimates[38] for μ^* for the components of the T_5T_9 alloys. Values for Θ_D were calculated from experimental measurements of Young's modulus Y, and the following expression[39]:

$$\Theta_D = \frac{h}{k_B}\left(\frac{9N}{4\pi}\right)^{1/3}\frac{Y^{1/2}}{\bar{M}^{1/3}\bar{d}^{1/6}}f_2(\sigma). \tag{5}$$

In Eq. (5) h is Planck's constant, N is Avogadro's number, $\bar{M}$ is the mean atomic weight, d is the density, and $f_2(\sigma)$ is a function of Poisson's ratio σ. If we assumed $\sigma \approx 0.40$, as commonly observed in amorphous alloys,[40] $f_2(\sigma) = 0.46$. The calculated values of Θ_D are listed in Table III. They are approximately 25% lower than the weighted average of Θ_D of the respective elements which make up the T_5T_9

TABLE III. Calculated values for λ and $N(E_F)$.

Alloy	T_c (K)	Θ_D (K)	λ ($\mu^*=0.1$)	λ ($\mu^*=0.15$)	$\bar{\lambda}$[a]	$N(E_F)$ (states eV^{-1} at.$^{-1}$)
$Nb_{55}Rh_{45}$	5.13	273	0.60	0.71	0.65	1.04
$Nb_{55}Ir_{45}$	4.88	253	0.60	0.72	0.62	0.85
$Ta_{55}Rh_{45}$	3.37	247	0.54	0.65	0.56	0.73
$Ta_{55}Ir_{45}$	3.39	232	0.55	0.66	0.52	0.64

[a]$\bar{\lambda}$ is the weighted average of the λ's for the components.

alloys. Debye temperatures approximately 30% lower than the average of Θ_D of the component elements have been directly measured by low-temperature specific heat ($Cu_{57}Zr_{43}$) or estimated from $\rho(T)$ data (NbNi) for similar amorphous alloys.[41]

The λ was calculated from Eq. (4) using the calculated Θ_D values and $\mu^*=0.1$ and 0.15. The results are listed in Table III. It is apparent that the T_5T_9 amorphous alloys are "intermediate-coupled" superconductors. The λ values for $Nb_{55}Rh_{45}$ and $Nb_{55}Ir_{45}$ are essentially identical as are those for $Ta_{55}Ir_{45}$ and $Ta_{55}Rh_{45}$. If $\mu^*=0.15$ is assumed, λ for the T_5T_9 alloys containing Ta is identical with λ for pure Ta while the λ's for the T_5T_9 alloys containing Nb are less than λ for pure Nb ($\lambda=0.92$). Values for λ calculated by taking the weighted average of the λ's for the elements constituting the T_5T_9 alloys are also given in Table III and it is noted that they are comparable to the values determined from the T_c and Θ_D data.

3. *Calculation of the density of states $N(E_F)$*

With values of γ and λ it is then possible to calculate $N(E_F)$. The $N(E_F)$ values are listed in Table III in the conventional units of states per eV atom. Density of states obtained this way, modified by the electron-phonon enhancement factor $(1+\lambda)$, have been found to agree reasonably well with first principle band-structure calculations for transition-metal elements.[26,37]

G. Variation of T_c with γ, $N(E_F)$, and λ

Values of γ were calculated from the GLAG expression [Eq. (3)] for the amorphous Ta-Rh alloys. Neither γ nor T_c show appreciable variation with e/a. In Fig. 10 T_c is plotted against γ for $(Nb_{1-x}Ta_x)_{55}Ir_{45}$ and $(Nb_{1-x}Ta_x)_{55}Rh_{45}$. A strong dependence of T_c on γ is seen with separate curves for the alloys containing Ir and Rh. That is, even though the alloys with Rh have higher values of γ than those containing Ir for a given Nb/Ta ratio, i.e., value of x, the T_c values are similar for the two systems. Since λ data are only available for the four T_5T_9 alloys ($x=0$ or 1), $N(E_F)$ could only be calculated for these. T_c vs $N(E_F)$ for the four alloys is illustrated in Fig. 11. Figure 11 resembles the T_c vs γ plot of Fig. 10 since $(1+\lambda)$ does not markedly change the values calculated for $N(E_F)$ from γ. The dotted lines connecting the data for the Ir- and Rh-containing alloys indicate the expected behavior following the behavior of γ in Fig. 10. Thus, the Nb/Ta ratio controls T_c even though Ir and Rh provide different density-of-states values.

Therefore, $N(E_F)$ alone must not be controlling T_c in the amorphous T_5T_9 alloys. The λ appears to reflect the T_c behavior more accurately than $N(E_F)$. For example, in $Ta_{55}Ir_{45}$ and $Ta_{55}Rh_{45}$ where the T_c values are nearly identical, the λ values only differ by approximately 1%, while the value for $N(E_F)$ is about 15% greater for $Ta_{55}Rh_{45}$ than for $Ta_{55}Ir_{45}$.

The electron-phonon coupling parameter can be

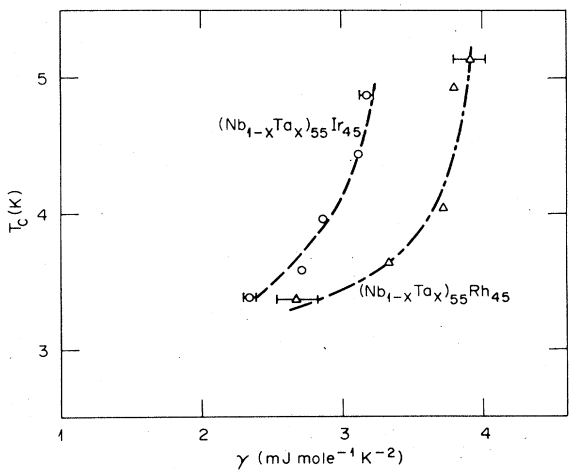

FIG. 10. Superconducting transition temperature, T_c vs γ.

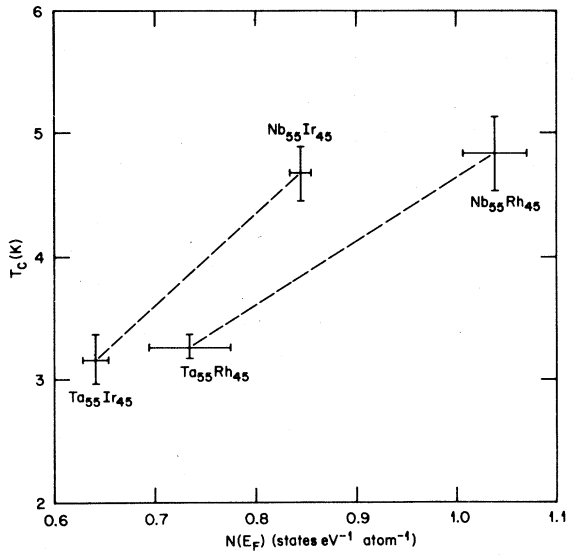

FIG. 11. Superconducting transition temperature, T_c vs $N(E_F)$.

expressed as[37]

$$\lambda = \frac{N(E_F)\langle I^2\rangle}{M\langle\omega^2\rangle} \quad , \tag{6}$$

where $\langle I^2\rangle$ is the squared average electron-phonon matrix element, M is the atomic mass, and $\langle\omega^2\rangle$ is the squared average phonon frequency which has often been estimated by Θ_D^2. In certain classes of materials, including recent results on amorphous lanthanum-base alloys,[42] it has been found that $\langle I^2\rangle/M\langle\omega^2\rangle$ is a constant and variations in λ are due to changes in $N(E_F)$. This behavior is not observed in the T_5T_9 alloys where $\langle I^2\rangle/M\langle\omega^2\rangle$ increases by 50% from $Nb_{55}Rh_{45}$ to $Ta_{55}Ir_{45}$. The numerator $N(E_F)\langle I^2\rangle$, which can be considered the "electronic" term, does not vary consistently with λ or T_c, but does change by up to 27%, so it cannot be considered constant. The denominator, the "phonon term," also varies in the T_5T_9 alloys, by as much as 38%. The λ for a given T_5T_9 alloy is thus determined by both the electronic and phonon properties.

An additional possible influence on T_c in these T_5T_9 alloys is the very short mean free path for electrons. Meisel and Cote[43] have recently suggested that the Pippard and Ziman[44] condition on electron-phonon interactions can depress T_c. This condition states that phonons whose wavelengths exceed the electron mean free path are ineffective electron scatterers. The entire phonon spectrum contributes to T_c. When the electron mean free path is short, the Pippard and Ziman condition introduces a residual-resistivity-dependent low-frequency cutoff on the phonon frequencies which contribute to T_c. The T_5T_9 amorphous alloys have high residual resistivities such that the Pippard and Ziman condition should apply. T_c is observed to decrease with increasing resistivity for these alloys but it is not clear how the mechanism suggested by Meisel and Cote can be separated from the other electronic and phonon contributions to λ and T_c.

H. $N(E_F)$ and amorphous phase stability

The relative stability of amorphous phases has been discussed in terms of atomic size,[45] electronic structure,[46,47] and structural complexity.[48] It would appear that a mixture of these effects controls stability in general, while certain alloy systems seem to be dominated by a given factor. As in crystalline materials, the stability problem is complex and as yet unresolved. Nagel and Tauc[47] have proposed a correlation of glass stability with e/a such that maximum stability occurs when $N(E_F)$ is a minimum. Analogous to the Ziman-Faber theory for resistivity, this will occur when $2K_F$, the "spanning vector" of the Fermi surface equals K_p, the position of the first maximum in the structure factor $S(k)$. Some experimental evidence as well as theoretical calculations[49,50] support this model while other experimental results[51] do not. Since we have calculated $N(E_F)$ for the T_5T_9 alloys it is interesting to find a suitable parameter for relative stability for which a comparison can be made. One such possible parameter is the ratio of the crystallization temperature (at a constant heating rate) to the melting temperature of the alloy, T_x/T_m. For the T_5T_9 alloys T_m corresponds to the eutectic temperature. In Fig. 12, T_x/T_m is plotted against

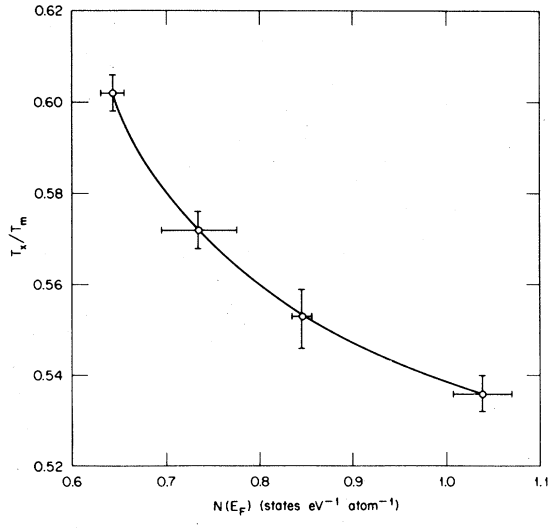

FIG. 12. T_x/T_m vs $N(E_F)$, with T_x = temperature of crystallization and T_m = melting temperature.

$N(E_F)$ with T_x determined at 10 °C/min and T_m obtained from the equilibrium phase diagrams.[8] If T_x/T_m is a suitable parameter for measuring the amorphous phase stability, it is clear that the stability of the T_5T_9 amorphous alloys increases with decreasing $N(E_F)$. This is consistent with the Nagel and Tauc model and the resistivity results discussed in Sec. III E.

A generally linear relationship has been found between T_x and NTC in $(Fe_{0.5}Ni_{0.5})_{100-x}B_x$ alloys.[52] It was suggested that these results provide strong evidence that an electronic contribution to the stability of metallic glasses exists. Similarly, in the present work an essentially linear relationship is found between T_x (or T_x/T_m) and NTC. This gives further support for the above suggestion.

IV. SUMMARY AND CONCLUDING REMARKS

The superconducting transition temperature has been measured in a number of T_5T_9 amorphous alloys as a function of composition. Changing the composition within a given T_5T_9 alloy had little effect on T_c. Substituting Ta for Nb at a constant T_9 composition decreased T_c, with T_c dropping almost linearly with x in $(Nb_{1-x}Ta_x)_{55}Ir_{45}$ and $(Nb_{1-x}Ta_x)_{55}Rh_{45}$.

From the superconducting measurements, T_c and $dB_{c2}/dT|_{T_c}$, and the resistivity, a value for γ could be calculated using the GLAG theory. The γ values were used to estimate $N(E_F)$ using λ calculated from Θ_D, which was determined by elastic constant measurements. Comparing T_c with $N(E_F)$ and λ as a function of composition indicated that λ reflects the T_c behavior more closely. That is, both T_c and λ appear to be dominated by Nb and Ta while $N(E_F)$ does depend on the T_9 component. Examination of the quantities which determine λ indicates that both the electronic and phonon terms must be considered. It would be useful to have more direct measurements of $N(E_F)$ in these alloys, for example from low-temperature specific-heat capacity experiments. Then the calculated γ values could be confirmed, and more confidence could be placed on the above discussions.

The resistivity and negative coefficients of resistivity are consistent with the Ziman-Faber model. The increase in resistivity with Ta concentration may be rationalized by the stronger scattering of electrons from the Ta d bands.

If T_x/T_m is considered as a measure of glass stability, then to the extent that T_x/T_m decreases with $N(E_F)$, the present data are consistent with the model of Nagel and Tauc.

ACKNOWLEDGMENTS

The authors would like to thank G. M. Stocks for the theoretical interpretation of the resistivity data. Thanks are also given to O. B. Cavin for the x-ray-diffraction measurements, W. H. Butler and A. DasGupta for reviewing the manuscript. Research sponsored by the Division of Material Sciences, U. S. Department of Energy under Contract No. W-7405-eng-26 with the Union Carbide Corporation.

[1]W. L. Johnson, S. J. Poon, and P. Duwez, Phys. Rev. B 11, 150 (1975); W. L. Johnson and S. J. Poon, J. Appl. Phys. 46, 1787 (1975).
[2]P. Duwez and W. L. Johnson, J. Less Common Met. 62, 215 (1978).
[3]W. L. Johnson, in *Rapidly Quenched Metals III,* edited by B. Cantor (The Metals Society, London, 1978), Vol. 2, p. 1.
[4]O. Rapp, B. Lindberg, H. S. Chen, and K. V. Rao, J. Less Common Met. 62, 221 (1978).
[5]W. Buckel and R. Hilsch, Z. Phys. 138, 109 (1954).
[6]M. Fischer, D. E. Polk, and B. C. Giessen, in *Rapid Solidification Processing: Principles and Technologies,* edited by R. Mehrabian, B. H. Kear, and M. Cohen (Claitors, Baton Rouge, 1978), p. 140.
[7]*Constitution of Binary Alloys,* edited by F. A. Shunk (McGraw-Hill, New York, 1969), 2nd supplement, pp. 187, 197, 463, 644.
[8]M. M. Collver and R. H. Hammond, Phys. Rev. Lett. 30, 92 (1973).
[9]M. M. Collver and R. H. Hammond, Solid State Commun. 22, 55 (1977).
[10]W. L. Johnson and S. J. Poon, J. Appl. Phys. 46, 1787 (1975).
[11]S. H. Whang, L. T. Kabacoff, D. E. Polk, and B. C. Giessen, J. Mater. Sci. 15, 247 (1980).
[12]B. C. Giessen and C. M. J. Wagner, in *Liquid Metals, Chemistry and Physics,* edited by S. Z. Beer (Marcel Dekker, New York, 1972), p. 654.
[13]A. Guinier, *X-Ray Diffraction* (Freeman, San Francisco, 1963), p. 72.
[14]S. Davis, M. Fischer, B. C. Giessen, and D. E. Polk, in *Rapidly Quenched Metals III,* edited by B. Cantor (The Metals Society, London, 1978), Vol. 2, p. 425.
[15]E. Bucher, F. Heiniger, and J. Muller, Helv. Phys. Acta 34, 843 (1961).
[16]C. C. Koch and J. O. Scarbrough, Phys. Rev. B 3, 742 (1971).
[17]V. Sadagopan and H. C. Gatos, Phys. Status Solidi 13, 423 (1966).
[18]R. D. Blaugher and J. K. Hulm, J. Phys. Chem. Solids 19, 134 (1961).
[19]W. L. Johnson and S. J. Poon, J. Less Common Met. 42, 355 (1975).
[20]W. L. Johnson and A. R. Williams, Phys. Rev. B 20, 1640 (1979).
[21]R. R. Hake, Phys. Rev. B 158, 356 (1967).
[22]T. E. Faber and J. M. Ziman, Philos. Mag. 11, 153 (1965).
[23]O. Dreirach, R. Evans, H. J. Güntherodt, and H. U. Kun-

zi, J. Phys. F 2, 709 (1972).
[24]G. M. Stocks (private communication).
[25]D. Papaconstantopoulos and B. Klein, private communication to W. H. Butler; also see L. L. Boyer, D. A. Papaconstantopoulos, and G. M. Klein, Phys. Rev. B 15, 3685 (1977).
[26]L. F. Mattheiss, Phys. Rev. B 1, 373 (1970).
[27]E. Esposito, H. Ehrenreich, and C. D. Gelatt, Jr., Phys. Rev. B 18, 3913 (1978).
[28]C. C. Koch, G. M. Stocks, and A. H. Narten (unpublished).
[29]G. Bergmann, Phys. Rev. B 7, 4850 (1973).
[30]R. Koepke and G. Bergmann, Solid State Commun. 19, 435 (1976).
[31]B. R. Coles, in *Transition Metals 1977,* edited by W. J. G. Lee, J. M. Perz, and E. Fawcett, IOP Conf. Proc. No. 39 (IOP, Bristol and London 1978), p. 180.
[32]T. P. Orlando, E. J. McNiff, Jr., S. Foner, and M. R. Beasley, Phys. Rev. B 19, 4545 (1979).
[33]W. H. Shull, D. G. Naugle, S. J. Poon, and W. L. Johnson, Phys. Rev. B 18, 3263 (1978).
[34]W. H. Shull and D. G. Naugle, Phys. Rev. Lett. 39, 1580 (1977).
[35]S. Nanao, Y. Ohji, J. Sugiura, and H. Ino, in *Rapidly Quenched Metals III,* edited by B. Cantor (The Metals Society, London, 1978), Vol. 2, p. 48.
[36]W. L. Johnson, S. J. Poon, J. Durand, and P. Duwez, Phys. Rev. B 18, 296 (1978).
[37]W. L. McMillan, Phys. Rev. 167, 331 (1968).
[38]K. H. Bennemann and J. W. Garland, in *Superconductivity in d- and f-Band Metals* —1972, edited by D. H. Douglass, AIP Conf. Proc. No. 4 (AIP, New York, 1972), p. 116.
[39]F. H. Herbstein, Adv. Phys. 10, 318 (1961).
[40]H. S. Chen and K. A. Jackson, in *Metallic Glasses,* edited by H. J. Leamy and J. J. Gilman (American Society for Metals, Metals Park, Ohio, 1978), p. 84.
[41]S. R. Nagel, J. Vassiliou, P. M. Horn, and B. C. Giessen, Phys. Rev. B 17, 462 (1978).
[42]K. Agyeman, R. Müller, and C. C. Tsuei, Phys. Rev. B 19, 193 (1979).
[43]L. V. Meisel and P. J. Cote, Phys. Rev. B 19, 4514 (1979).
[44]A. B. Pippard, Philos. Mag. 46, 1104 (1955); J. M. Ziman, *Electrons and Phonons* (Clarendon, Oxford, 1960), Chap. 5.
[45]D. E. Polk, Acta Metall. 20, 485 (1972).
[46]H. S. Chen and B. K. Park, Acta Metall. 21, 395 (1973).
[47]S. R. Nagel and J. Tauc, Phys. Rev. Lett. 35, 380 (1975); J. Tauc and S. R. Nagel, Comments Solid State Phys. 7, 69 (1976).
[48]R. Wang, Nature 278, 700 (1979).
[49]H. Beck and R. Oberle, in *Rapidly Quenched Metals III,* edited by B. Cantor (The Metals Society, London, 1978), Vol. 1, p. 416.
[50]J. Hafner and L. von Heimendahl, Phys. Rev. Lett. 42, 386 (1979).
[51]T. B. Massalski, U. Mizutani, K. T. Hartwig, and R. W. Hopper, in *Rapidly Quenched Metals III,* edited by B. Cantor (The Metals Society, London, 1978), Vol. 2, p. 81.
[52]H. Hillmann and H. R. Hilzinger, in *Rapidly Quenched Metals III,* edited by B. Cantor (The Metals Society, London, 1978), Vol. 1, p. 371.